The Holocene 16,8 (2006) pp. 1137–1147

Seasonal and subseasonal climate changes recorded in laminated diatom ooze sediments, Adélie Land, East Antarctica

D. Denis,[1]* X. Crosta,[1] S. Zaragosi,[1] O. Romero,[2] B. Martin[1] and V. Mas [1–3]

([1]UMR-CNRS 5805 EPOC, université Bordeaux 1, av. des Facultés, 33405 Talence cedex, France; [2]Department of Geosciences and RCOM, University of Bremen, PO Box 330440, 28334 Bremen, Germany; [3]IFREMER, Géosciences Marines, Laboratoire Environnements Sédimentaires, BP70, 29280 Plouzané Cedex, France)

Received 16 January 2006; revised manuscript accepted 6 June 2006

A HOLOCENE RESEARCH PAPER

Abstract: A 40 m long sediment core covering the 1000–9600 years BP period was retrieved from the Dumont d'Urville Trough off Adélie Land, East Antarctica, during the MD 130-*Images* X-CADO cruise. This sedimentary sequence allows the documentation of changes in climate seasonality during the Holocene. Here we show preliminary results of diatom communities, lithic grain distribution and titanium content measured on two 30 cm long sequences of thin sections. The two sequences originate from two different climate regimes, the colder Neoglacial and the warmer Hypsithermal. Proxies were measured at microscale resolution on 25 laminations for the Neoglacial and 14 laminations for the Hypsithermal. The two sequences reveal alternating light-green and dark-green laminae. Light laminae result from low terrigenous input and high sea-ice edge diatom fluxes and are interpreted to represent the spring season. Dark laminae result from high terrigenous input mixed with a diversified open ocean diatom flora and are interpreted to represent the summer–autumn season. The two sequences therefore resolve annual couplets composed of one light plus one dark lamina. Variations in the relative thickness of laminations and annual couplets, associated with diatom assemblage changes, are observed in each sequence and between the two sequences giving information on interannual to millennial changes in environmental conditions.

Key words: Adélie Land, Holocene, laminated sediments, diatom ooze, seasonality, sea ice, East Antarctica.

Introduction

Based on ice core records (Masson *et al*., 2000; NGICP members, 2004), the Holocene period was believed rather stable in comparison with the last glacial period. However recent palaeo-oceanographic investigations have revealed rapid and large amplitude variations in the North Atlantic (de Menocal *et al*., 2000; Bond *et al*., 2001) and in the Southern Ocean (Hodell *et al*., 2001; Nielsen *et al*., 2004). Sites of high sediment accumulation are therefore necessary to document these variations and to understand their frequency and origin. In that perspective, Antarctic inner shelf basins that present laminated sediments allow annual to subseasonal reconstructions of Holocene oceanographic and climatic conditions, which may help to understand better both the interactions between Antarctic atmospheric–oceanic–cryospheric–sea-ice processes, deep ocean circulation and teleconnections between high and low latitudes. Most of the studies aimed at deciphering the signal recorded in laminations originate from the Antarctic Peninsula (eg, Pike *et al*., 2001; Leventer *et al*., 2002; Bahk *et al*., 2003; Maddison *et al*., 2005) and the Mac Robertson Shelf (Stickley *et al*., 2005). Nonetheless, evidence for strong Antarctic regional heterogeneities in recent climate changes (Jones *et al*., 1993; King *et al*., 2003) call for additional sedimentary records in order to provide a more comprehensive view of past climate dynamics at high southern latitudes. The Adélie Land region in the East Antarctica Margin (EAM) has received little attention so far, despite evidences for very high sediment accumulation (Leventer *et al*., 2006). Core MD03-2601 from the Dumont d'Urville Trough is a 40 m long sequence of laminated diatom ooze that covers the Holocene. Investigation of diatom communities, lithic grain distribution and titanium content at microscale resolution on two 30 cm long laminated sequences aimed to document (1) the nature of

*Author for correspondence (e-mail: d.denis@epoc.u-bordeaux1.fr)

10.1177/0959683606069414

the signal preserved in the laminations and (2) whether laminations may be used here to track climate change at the interannual timescale.

Oceanographic setting

The SE–NW oriented Dumont d'Urville Trough off Adélie Land is located on the EAM (Figure 1). It is composed of a succession of glacial depressions enclosed between the Dibble Bank to the west and Adélie Bank to the East. Core MD03-2601 (66°03.07′S; 138°33.43′E; 746 m water depth) was recovered from the slope of a small depression located ~60 km off the Adélie Land coast. This region is influenced by three water masses (Bindoff *et al*., 2001): the Antarctic Coastal Current (ACC), which flows westward at the surface (Figure 1); the Modified Circumpolar Deep Water (MCDW), which upwells at the Antarctic Divergence; and the High Salinity Shelf Water (HSSW) formed by brine-rejection during winter sea ice formation and cooling of the MCDW, which flows northward as part of the Antarctic Bottom Water (AABW) (Harris, 2000). The Adélie Land region is dissected by several small glaciers (Figure 1) injecting fresh water and terrigenous particles in the coastal area although these small glaciers have much less influence than the larger Mertz Glacier located few degrees to the East (Escutia *et al*., 2003). Sea ice is present ~9 months per year over the core site (Schweitzer, 1995) with more open marine conditions between January and March. Sea ice advances rapidly from April to June to reach its maximum extension between July and September, then retreats slowly during spring melting to attain its minimum extent during February. The Marginal Ice Zone is believed to be macro- and micronutrient rich, and ice melting produces a stratified stable environment favourable for diatom blooms (Leventer, 1992).

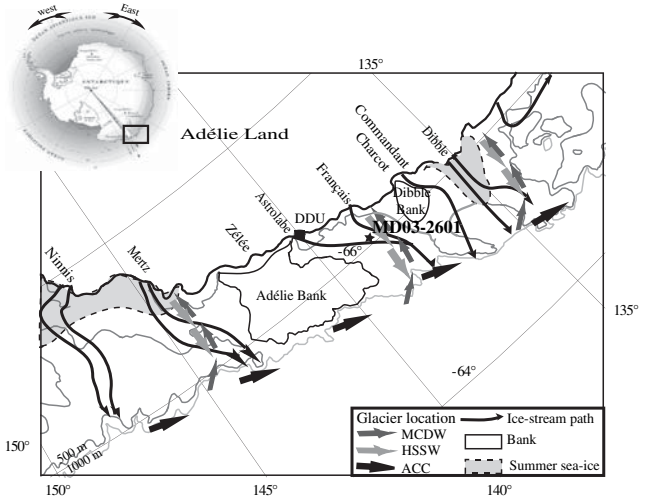

Figure 1 Location of core MD03-2601, limit of summer sea ice cover (Schweitzer, 1995), location of glaciers and ice-streams (Massom *et al*., 1998; Escutia *et al*., 2003), detail of oceanographic currents and different water masses (Harris and Beaman, 2003). DDU, Dumont d'Urville Base; ACC, Antarctic Coastal Current; MCDW, Modified Circumpolar Deep Water; HSSW, High Salinity Shelf Water. Winter sea ice covers the whole oceanic area encompassed by the map

Material and methods

Material and core stratigraphy

Core MD03-2601 was collected using the MDII Calypso piston corer during the MD130-*Images* X-CADO cruise in 2003. This 40.24 m long sequence of diatom ooze alternates between laminated and massive facies, and does not show any obvious visual disturbance. Stratigraphic control is based on five AMS ^{14}C dates on humic acid (Crosta *et al*., 2005) that were subsequently corrected by a marine reservoir age of 1300 years (Ingólfsson *et al*., 1998). The core covers the period from 9600 to 1000 yr BP. Diatom census counts and δ^{15}N and δ^{13}C investigations (Crosta *et al*., 2005) have shown that the Holocene period off Adélie Land can be divided into two different climatic phases: a colder Neoglacial (after 4000 yr BP), and a warm Hypsithermal (4000–9600 yr BP), which contains a cooling event (6350–8000 yr BP).

Laboratory procedures

Laboratory procedures involve preparations for macroscale investigations on half-core sections and for microscale analyses on thin sections.

Titanium content (Ti) expressed in counts per second (cps) was measured on half-core sections at 2 cm spacing along the entire core and at 2 mm spacing on the studied sections, on the Bremen University CORTEX XRF core-scanner following Jansen *et al*. (1998) method. Daily calibration of the XRF core-scanner precluded drift over time, thus ensuring low standard deviations of the data. Titanium is believed to be of terrigenous origin as this element does not participate in biological and diagenetic cycles, in contrast to iron and aluminium (Taylor and McLennan, 1985; Yarincik and Murray, 2000). Aluminium, which is actively uptaken and accumulated by diatoms, cannot be applied here to normalize Ti values (Van Bennekom *et al*., 1989; Moran and Moore, 1992).

Positive x-ray pictures of half-core sections were done using the SCOPIX image-processing tool (Migeon *et al*., 1999). Variations in grey levels indicate changes in the sediment density and thus composition. The light and dark laminations observed here correspond to sediment layers of low and high density, respectively.

Based on x-ray pictures, we determined the distribution and thickness of laminations along the entire core (Figure 2). We used a slightly modified technique from Francus *et al*. (2002), which involves drawing a suite of ellipses representative of each lamina and calculation of the distribution and thickness of laminae based on the ellipses in Scion Image®. This technique was applied to laminae only because sublaminae are difficult to distinguish on x-ray pictures. This approach helped us to sample two ~30 cm long sections of continuously laminated sediment. Section 5 (619–648.5 cm) originates from the Neoglacial while section 13 (1880.8–1910.7 cm) comes from the Hypsithermal.

Each lamina observed on x-ray pictures from sections 5 and 13 was sampled for diatom census counts and bulk isotopic ratios. Permanent slides were mounted following the procedure of Rathburn *et al*. (1997). This sampling strategy that takes the sediment over the entire thickness of the half-core sections cannot give access to diatom successions at the lamination scale because laminae are here inclined in both the horizontal and vertical plains. Such diatom census counts are, however, essential to interpret diatom assemblages at microscale on the thin sections.

Three thin sections (TS) were made for each period (TS 1, 2, 3 for core section 5 and TS 4, 5, 6 for core section 13) using the impregnating method detailed in Zaragosi *et al*. (2006).

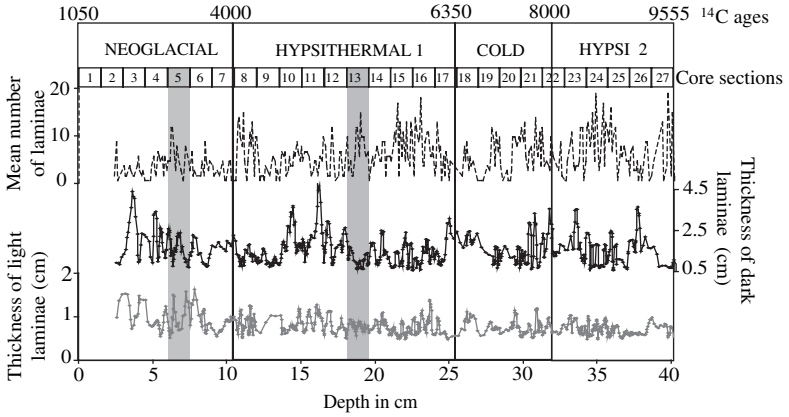

Figure 2 Mean number of laminations per 10 cm intervals (dashed line) and thickness of dark (black line) and light (grey line) laminations versus depth. Laminae thicknesses are smoothed with a 50 cm running average. Core sections, climatic periods and ^{14}C dates are reported at the top. The location of the studied sections 5 and 13 is represented by shaded zones

The goal of this technique is to embed a large sediment volume into a permanent medium without disturbing the sediment structure. The resulting thin sections (TS) are used here to document variations in the biogenic and lithogenic content.

Optical observations were conducted on the TS using an Olympus BH2 light microscope at magnification of 250 × and 500 × to determine diatom community changes with a focus on the relative importance of dominant species. Diatom census counts along the entire core (Crosta *et al.*, 2005) and within each lamina over the studied sections give us complementary insight on diatom assemblages and dominant species at decacal to subdecadal scales, which ascertains diatom identification on the TS.

Detrital material was similarly studied on the TS to determine (1) the mineral type via polarized light and (2) the distribution and number of lithics particles as grain number per square millimetre using an imagery system composed of a LEICA DM600B Digital microscope and Leica QWin 3.0 software. We conducted image analysis on 2.5–3.5 cm^2 TS areas, later referred to as Photomosaic (PM) (see Figure 4). Because of the homogeneous amorphous matrix of the diatom ooze sediment and of the impregnating Epoxy resin, the sediment matrix appeared darker than the clastic grains in the analysed polarized light. The picture processing method, detailed in Francus (1998), counts all the grains present in the area and estimates several characteristics as surface, width and length of the lithic grain. Two slides (TS2 and TS3) with very cottony texture did not allow coherent image acquisition and were not used in the calculations.

Results

General observations

Because of the sediment composition, laminations are almost invisible to the naked eye on half-core sections. They are, however, visualized on x-ray images as light and dark layers and on TS as light and brown layers. We will hereafter refer to light and dark laminae, which together form a couplet.

Mean thicknesses of light and dark laminations are 0.7 cm ($n = 937$, $\sigma = 0.4$) and 1.12 cm ($n = 1018$, $\sigma = 1.22$), respectively (Figure 2). Light and dark lamination thickness and lamination number reveals no obvious trend with depth but rather cyclic variations, whereas thickness of light laminations shows a slight decrease with depth.

Generally, x-ray images and TS show gradational colour contact between a light lamina and the overlying dark lamina and sharp colour contact from a dark to the overlying light lamina. Microscopic observations on TS reveal that light laminations are mainly composed of biogenic debris whereas dark laminations are composed of a mixture of biogenic and detrital debris, the latter being mainly clay and silt. Petrographic observations indicate that the clastic grains are mainly quartz. Only observable on TS, thin light laminae, called sublaminae, are found in dark laminations.

Section 5: Neoglacial period

Twenty-five laminations and four sublaminations are distinguished on TS 1, 2 and 3 that represent a ~30 cm long sequence of undisturbed sediment within section 5 (see Figure 4a for TS location). These laminations include 12 lights, 11 darks and 2 transitional laminae with average thicknesses of 1.1 cm ($\sigma = 0.8$), 0.8 cm ($\sigma = 0.8$) and 0.4 cm ($\sigma = 0.03$), respectively. The mean thickness of a couplet reaches 2.1 cm ($n = 10$, $\sigma = 1.4$).

Diatom assemblages

Diatom census counts performed between 608 cm and 670 cm ($n = 50$) show few dominant species among a highly diverse diatom community (~50 species), thus confirming results from lower resolution diatom counts (Crosta *et al.*, 2005). In section 5, *Fragilariopsis curta* and *Chaetoceros* resting spores (CRS), mainly *Hyalochaete Chaetoceros neglectus*, represent the dominant species with 26% and 19%, respectively. They are accompanied by a set of subordinate species or species groups such as other cryophilic *Fragilariopsis* species (12%), *F. rhombica* (10%), *F. kerguelensis* (8%), large centric species thriving in cold waters (8%), *Thalassiosira antarctica* (6%), *Phaeoceros* vegetative cells (5%), *Corethron pennatum* + rhizosolenoid species (4%) and needle-like species mainly represented by *Thalassiothrix antarctica* (2%) (Figure 3a).

Qualitative examinations of diatom assemblages on the TS demonstrate the same dominant species as mentioned above. These investigations, however, show the fine distribution of the diatom species that was invisible in the stepwise sampling. As a general statement, diatom distribution follows the colour changes of the laminations with a gradational evolution in the assemblages from light to dark laminae and an abrupt change from dark to light laminae. A close investigation depicts the following five main diatom assemblages, labelled A-B for the ones occurring in the light laminae and D-E-F for the ones encountered in dark laminae (Figure 3a and see Figure 5).

Assemblage type A is characterized by a co-dominance of *F. curta* plus other cryophilic *Fragilariopsis* species and CRS

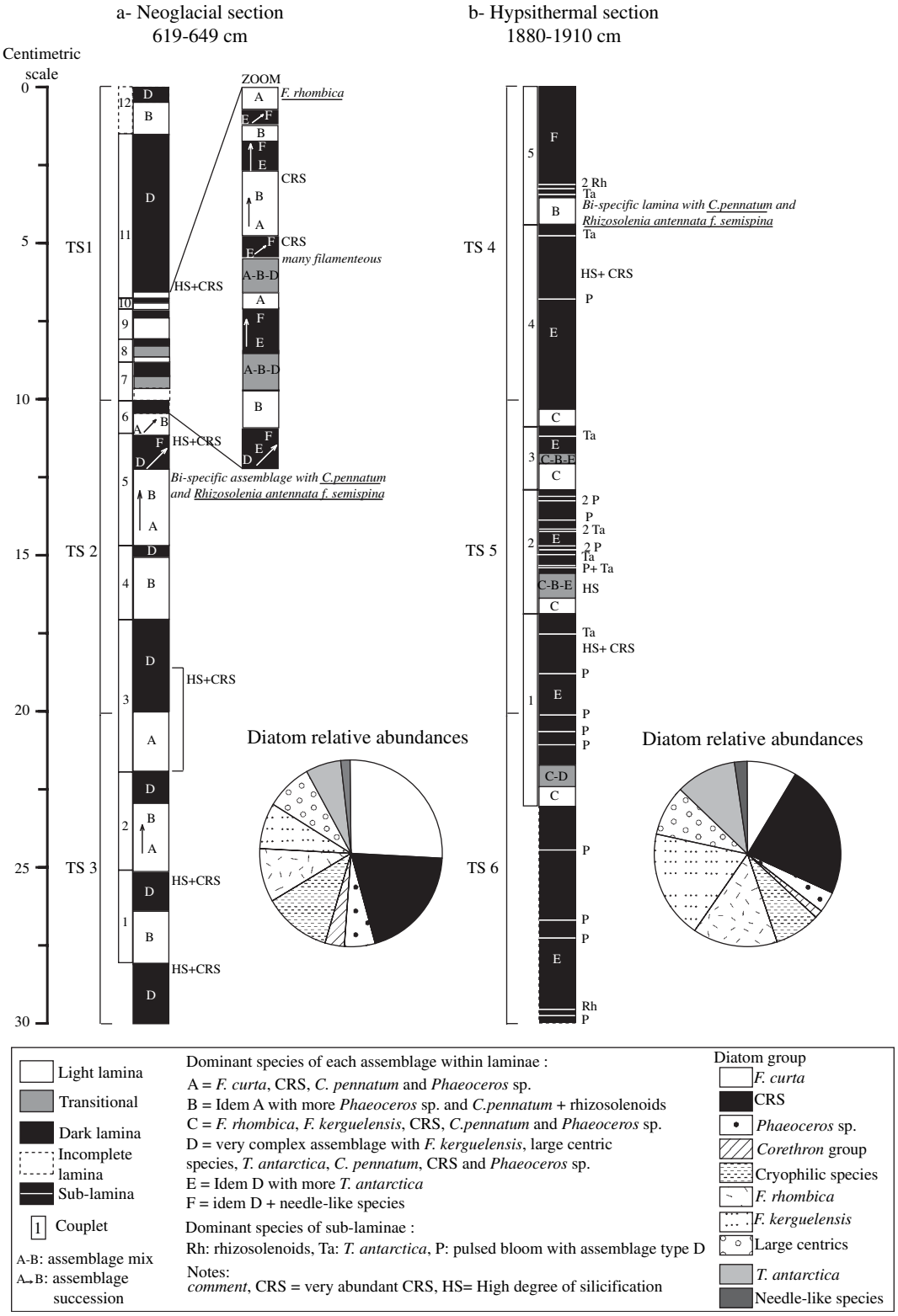

Figure 3 Schematic log of lamination and sublamination distribution in section 5 (a) and in section 13 (b). Location of the centimetric scale thin sections, and number of annual couplets are reported on the left side. Pie-charts illustrate the relative abundance of the various diatom groups from centimetric-scale diatom census counts in section 5 (a) and 13 (b)

plus vegetative *Phaeoceros* sp. and *C. pennatum*. *Chaetoceros* RS relative abundance increases progressively toward the top of the laminae while cryophilic *Fragilariopsis* species dominance decreases (Figure 3a). Assemblage type B is similar to assemblage type A with greater abundances of *C. pennatum*, rhizosolenoids and vegetative *Phaeoceros* sp. Assemblage type B becomes nearly bispecific in *C. pennatum* and rhizosolenoids in one occasion at the top of light lamination number five (Figure 3a). We counted 11 light laminae in the three TS of section 5, from which three laminae are characterized by assemblage type A, five laminae by assemblage type B and four laminae by a slow transition from assemblage type A to assemblage type B. The third and the ninth light laminae contained more CRS.

Assemblage type D shows a mixed flora composed of *F. kerguelensis*, CRS, *T. antarctica*, large centric species,

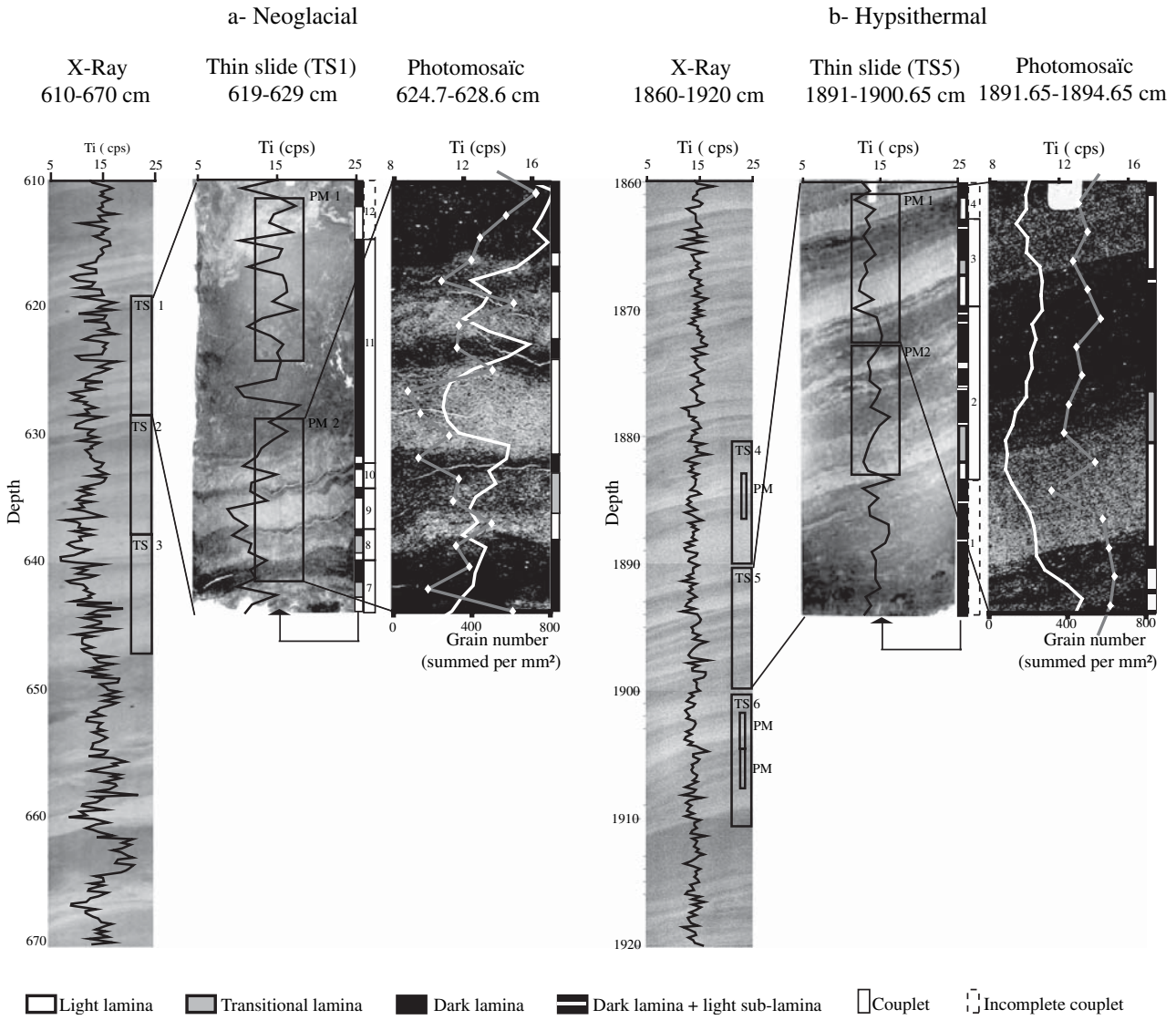

Figure 4 Location of the investigated sections on positive x-ray radiographs, thin sections and photomosaics for section 5 (a) and section 13 (b). Three thin sections (TS) were taken from each section. Two photomosaics (PM) were analysed in TS1 from section 5 while five photomosaics were analysed in the three TS from section 13. In each section, Ti content is visualized by the black curve. In the photomosaics, Ti content is represented by the grey curve with white points whereas the grain number per millimetre is illustrated by the white curve. Types of laminae and couplet succession are shown on the right of TS following the nomenclature depicted in Figure 3

Phaeoceros sp. and *C. pennatum*. Assemblage type E is similar to assemblage type D but with greater presence of *T. antarctica.* Assemblage type F also resembles assemblage type D but with a greater dominance of needle-like species (Figure 3a). We counted 11 dark laminations, from which seven are composed of the assemblage type D. The other dark laminations display a succession of assemblage types. Four laminations show a slow evolution from assemblage type E to assemblage type F, one lamination from assemblage type D to assemblage type F, and one lamination from assemblage type D to assemblage type E to assemblage type F (Figure 3a). Diatoms at the top of the dark laminations generally show a higher degree of silicification (see Figure 5). Complex dark laminations are encountered in couplets number five to ten in which light laminations also demonstrate a more complex structure. Transitional laminations between the light and the overlying dark lamination and showing a mixture of assemblage types A, B and D characteristics are also present here.

Detrital content

Titanium content is correlated to density changes visualized by x-ray photography with lower Ti content in light laminations than in dark laminations with mean values of 11.6 and 13.7 cps respectively (Figure 4a). Titanium content is similarly correlated to TS colour changes even though some variability is encountered within each lamina. We used the Wilcoxon-Mann-Whitney (WMW) test to determine whether the Ti content is significantly different in light and dark laminations. Briefly, the WMW is a non-parametric variance analysis test adapted for small data sets ($n_{light} = 45$, $n_{dark} = 47$, here) (Saporta, 1990). This test determines whether Ti values are randomly distributed or organized according to different populations (light and dark laminations). At the 1% confidence level, the WMW test yields a $H_{Ti\ content}$ value of 4.32 that is superior to the rejection threshold of 2.58. This demonstrates that different Ti content indeed prevails in light and dark laminations and that intracouplet differences are greater than homochromic intercouplet differences.

Determination of grain distribution and characteristics was only possible on TS 1 within two study zones: PM 1 and 2 (Figure 4a). The digital approach recognizes grains with diameter greater than 5 μm. In this population, silts are dominant with an unimodal histogram frequency centred at ~10 μm of diameter. In agreement with the Ti content data,

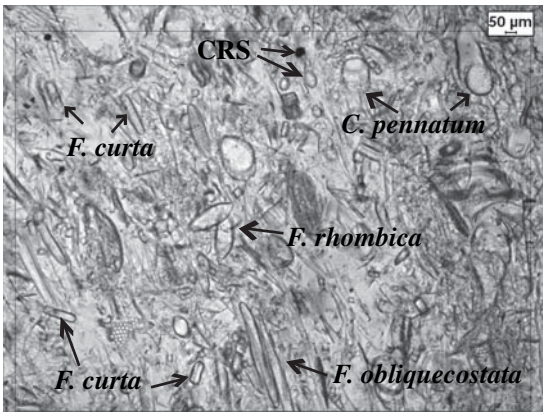

1. A type

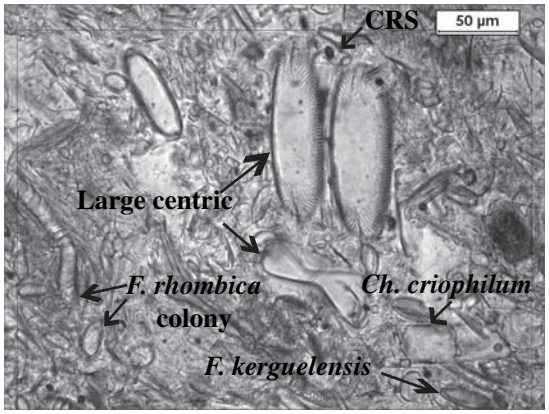

5. D type

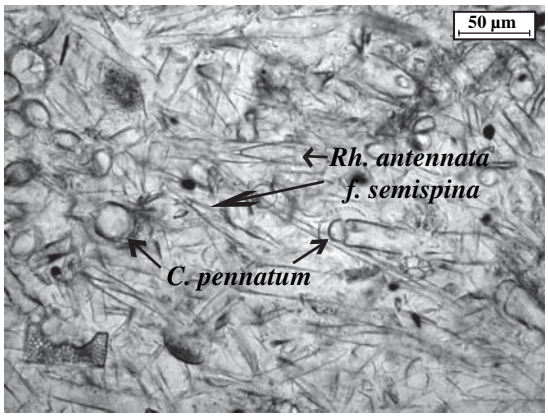

2. B type

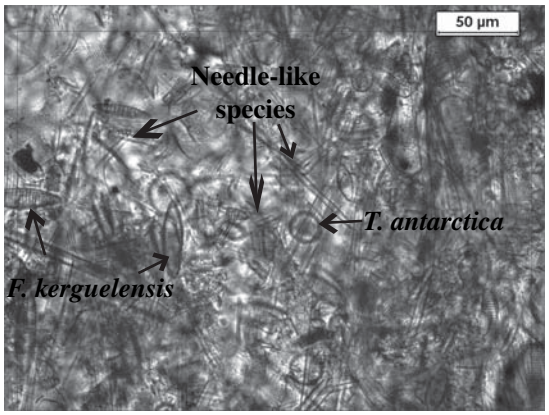

6. F type

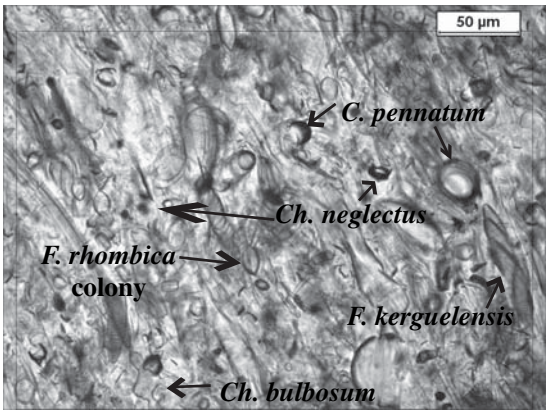

3. C type

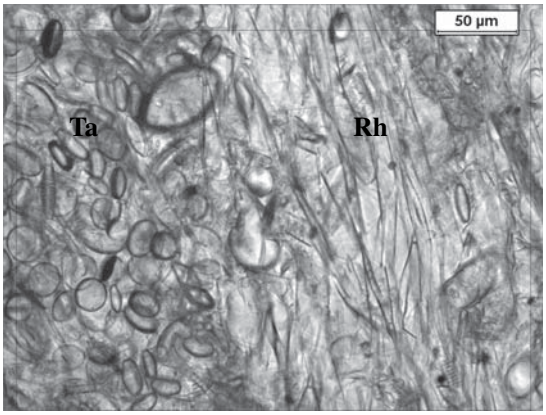

7. Ta and Rh sub-laminae

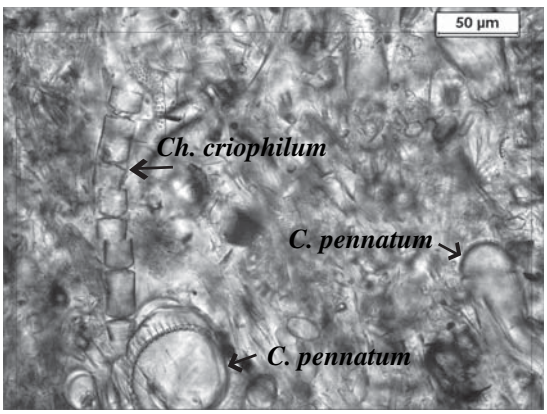

4. Low silicification degree

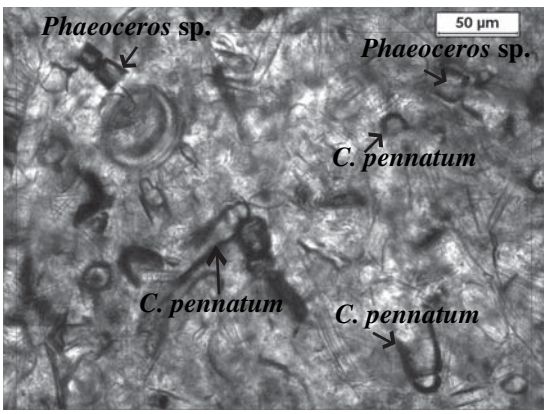

8. High silicification degree

Figure 5 Various diatom assemblage types. Photographs 1–3 and 5–6 show, respectively, typical light/biogenic laminae and dark/terrigenous laminae assemblages. Photograph 7 illustrates two types of sublaminae. Photographs 4 and 8 compare two different degrees of silicification on two diatom species

the number of lithic grains (GN) is generally lower in light ($n_{laminae} = 4$) than in dark laminae ($n_{laminae} = 5$) with mean values of 303 and 548 grains/mm^2, respectively (Figure 4a). We ascertained the significance of different grain populations in light versus dark laminations through the WMW statistic test. At the 1% confidence level, the WMW test yields a H_{GN} value of 2.84 superior to the rejection threshold of 2.58 ($n_{light} = 23$, $n_{dark} = 43$). Different GN thus prevails in light and dark laminations, indicating that intracouplet differences are greater than intercouplet differences between laminae of the same colour.

Section 13: Hypsithermal period

Fourteen laminations and 26 sublaminations were observed in section 13 (TS 4, 5, 6) (see Figure 4b for TS location). The laminations divide up into five lights, six darks and three transitional laminae with respective thicknesses of 0.7 cm ($\sigma =$ 0.1 cm), 3.6 cm ($\sigma = 1.8$ cm) and 0.6 cm ($\sigma = 0.2$ cm), yielding an average thickness of 4.6 cm ($\sigma = 1.6$) for the couplets. Thickness of sublaminae varies between 0.1 and 2.1 mm ($n =$ 26, mean = 1 mm, $\sigma = 0.6$ mm).

Diatom assemblages

Diatom census counts performed between 1858 cm and 1919 cm ($n = 62$) evidence the same diatom species as in section 5 but with an important shift in dominance. *Chaetoceros* resting spores (22%), *F. kerguelensis* (19%), *F. rhombica* (15%) and *T. antarctica* (11%) are more abundant and are accompanied by a suite of subordinate species such as large centric diatoms (9%), *F. curta* (9%), other cryophilic *Fragilariopsis* diatoms (8%), *Phaeoceros* vegetative cells (4%), needle-like species (2%) and *C. pennatum* and rhizosolenoids (1%) (Figure 3b).

Qualitative examinations of diatom assemblages on the TS demonstrate the same dominant species as mentioned above with a gradational evolution of the assemblages from light to dark laminae and an abrupt change from dark to light laminae. Three main assemblages are documented: assemblages type C in the light laminae and assemblages type E and F in the dark laminae (Figure 5).

Assemblage type C is mainly composed of *F. rhombica* associated with cryophilic *Fragilariopsis* sp., *F. kerguelensis* and CRS. The relative occurrence of CRS increases from bottom to top of the laminae. Out of five light laminations analysed on the TS taken from section 13, four are composed of assemblage type C. The last lamination is represented by the bi-specific assemblage type B defined before (Figure 3b).

Dark laminations are characterized by the above-described assemblage types E and F. Of six dark laminations, five are characterized by assemblage type E while the last lamination is composed of assemblage type F. We noted the presence of three transitional laminae, showing a mixture of assemblage types C, B and D in the lower part of the TS sequence (Figure 3b). We also noted that dark laminations numbers 1 and 4 present greater relative abundances of CRS and higher frustule silicification (Figure 5).

Twenty-six sublaminae appear as thin light laminae within dark laminations with upper and lower sharp contacts. Diatom examinations evidence three diatom assemblage types. Two are near monospecific assemblages, composed of *T. antarctica* ($n = 8$) or rhizosolenoids ($n = 3$) and referred to Ta and Rh, respectively (Figure 5). The last one, named P for pulsed event, is similar to assemblage type D ($n = 15$) (Figure 3b). The Rh sublaminae appear at the bottom of dark laminations while the Ta sublaminae generally occur at the top of dark laminations. P sublaminae are scattered throughout dark laminations. Ta, Rh and P display mean thicknesses of 371 μm ($\sigma = 289$ μm), 860 μm ($\sigma = 470$ μm) and 1300 μm ($\sigma = 460$ μm), respectively. These sublaminae cannot be interpreted as light laminations because of their specific diatom assemblages and reduced thickness. They conversely represent abrupt events during deposition of the dark laminations.

Detrital content

Ti relative concentrations are lower in light laminae than in dark laminae both at the x-ray and TS scale, with mean values of 13 and 14 cps, respectively (Figure 4b). Digital analysis of grains larger than 5 μm indicates dominance of the silt fraction with a unimodal histogram frequency centred at ~10 μm diameter. The number of grains (GN) calculated on 5 PM (Figure 4b) follows the same pattern as Ti content with mean values of 152 grains/mm^2 in light laminations and 264 grains/mm^2 in dark laminations. At the 1% confidence level, the WMW test yields a $H_{Ti\ content}$ value of 1.72, greater than the rejection threshold of 1.64, and a H_{GN} value of 5.61, also superior to the rejection threshold of 2.58 ($n_{light} = 25$, $n_{dark} =$ 111 for Ti content; $n_{light} = 58$, $n_{dark} = 94$ for GN). This demonstrates that different detrital populations prevail in light and dark laminations of the sequence studied here and that the intracouplet differences in Ti content and GN are greater than intercouplet differences of the same colour type lamination.

Discussion

The presence of well-preserved frustules of needle-like species and of the easily dissolved species *C. pennatum* (Beucher *et al.*, 2004) indicates that buried diatom communities are barely influenced by differential preservation and, thus, accurately record surface environment changes. We hereafter use data on detrital content as well as the ecological preferences of dominant species to determine the significance of lamination types and to link their succession to environmental conditions.

Seasonal and subseasonal signals

Light/biogenic laminae

Light laminae are characterized by low density, low Ti content and low GN. They are therefore mainly composed of biogenic material, ie, diatoms. Light laminae are characterized by assemblage types A and C in which cryophilic *Fragilariopsis* species (mainly *F. curta* in section 5 and *F. rhombica* in section 13) and CRS are the co-dominant species groups, with subordinate presence of *C. pennatum* and vegetative *Phaeoceros* sp.

Fragilariopsis curta and CRS show a preference for stable, stratified waters and sea ice proximity (Leventer, 1991; McMinn and Hodgson, 1993; Crosta *et al.*, 1997) that seeds the surrounding surface water as it melts. This seems also true for *F. rhombica*, with the difference that this species thrives in waters slightly warmer than *F. curta* (Armand *et al.*, 2005). These conditions are encountered in spring and, when associated with sufficient light and nutrients levels, promote intense diatom blooms. Blooms may eventually deplete the nutrient pool thus leading to CRS formation (Leventer, 1991). We therefore interpret the light/biogenic laminae to represent the spring season. Spring laminae evidence here, however, depart from previous studies in other cores from the EAM (Stickley *et al.*, 2005) and the Antarctic Peninsula (Leventer *et al.*, 2002; Bahk *et al.*, 2003; Maddison *et al.*, 2005) in which the spring season is characterized by greater abundances of CRS (60%). Low CRS occurrence is confirmed by diatom census counts all core long (Crosta *et al.*, 2005) and may result from more oceanic conditions prevailing at the core location.

Indeed, presence of *Phaeoceros* vegetative cells suggests an oceanic influence (Maddison, 2005) and *Ch. neglectus* has not been reported to be seeded from sea ice (Garrison *et al*., 1987; Riaux-Gobin *et al*., 2003).

Assemblage type A may be followed by the predominance of migrant species such as *C. pennatum* and rhizosolenoids that characterize the diatom assemblage type B. These species thrive normally in open water with little sea ice during the growing season (Fryxell and Hasle, 1971) and display positive buoyancy (Crawford, 1995; Leventer *et al*., 2002; Bahk *et al*., 2003). Out of Antarctica, these species groups were shown to be part of the shade flora that reaches very high biomass at the pycnocline (Kemp *et al*., 1999). Their record in the sediment was interpreted as an event of rapid sedimentation when the pycnocline weakened (Kemp *et al*., 2000). Increasing occurrence of *C. pennatum* and rhizosolenoids throughout the light laminae suggest here a strengthening of the pycnocline during the spring season, thus conducting to increasing biomass accumulation and export after cell senescence. This assemblage therefore may be an indicator of warmer, more oligotrophic, open-water intrusion (Stickley *et al*., 2005) or reduced wind stress.

The diatom succession from cryophilic *Fragilariopsis* species to CRS and finally to migrant species observed here indicates a transition from a cold-stratified environment with extensive sea ice cover at the beginning of the spring season to more open water as temperatures rise, with increasing seasonal insolation coupled to a decrease of the nutrient pool. Sea ice persistence implies low terrigenous input from the continent, which is additionally diluted by the intense diatom fluxes to the sea floor.

Dark/terrigenous laminae

Dark laminae are characterized by higher density, higher Ti content and higher GN. They are composed of a mixture of biogenic and terrigenous material. Dark laminae are characterized by more diverse diatom assemblages dominated by *F. kerguelensis*, *T. antarctica* and large centric species. These species preferentially thrive in open ocean water and do not support sea ice presence during the growing season (Armand *et al*., 2005; Crosta *et al*., 2005). They also exhibit lower nutrient requirements and lower growth rates than bloom-related species (Leventer and Dunbar, 1987; Zielinski and Gersonde, 1997). We interpret these assemblages as representative of summer production in open water when sea ice has retreated and nutrient levels are low, in agreement with previous studies conducted in the EAM (Leventer *et al*., 2002; Bahk *et al*., 2003; Maddison, 2005; Stickley *et al*., 2005).

Corethron pennatum and *Phaeoceros* vegetative cells are less abundant than in light laminae but display larger size and a higher degree of silicification, indicating a slow biomass build-up during the summer months. At the end of the summer season, the presence of needle-like species may become predominant, forming the assemblage type F. Here again, they may indicate the return of atmospheric perturbations during autumn that disrupt the pycnocline thus exporting downward the shade flora slowly growing at the nutricline (Bahk *et al*., 2003).

Both Neoglacial and Hypsithermal sections display greater GN and Ti content in dark laminations than in light laminations, suggesting higher terrigenous input during dark laminae deposition. In our study area, lithogenic input may have several sources including aeolian dust, focusing by deep currents (Presti *et al*., 2003), glacial runoff and subglacial melting (Rignot and Jacobs, 2002). The aeolian source, even with melting dirty sea ice, cannot account for the terrigenous fraction based on its timing. Indeed one would expect greater deposition during spring when sea ice decay releases dust particles. Strong winnowing that transports diatom frustules along with the detrital particles is not coherent with the seasonal and subseasonal signature of diatom assemblages. We therefore suggest that glacial and subglacial inputs are the dominant detrital sources to our core site and occur mainly during the summer/autumn season before the return of sea ice. Material input is primarily controlled by the extent and persistence of sea ice cover with secondary influence of atmospheric conditions. This inferred seasonal cycle in the detrital supply may be affected by the diluting effect of rapid and intense biogenic settling events.

The described sedimentary record preserves the imprint of seasonal and subseasonal biological and sedimentological dynamics, with biogenic laminae representing spring fluxes and more terrigenous laminae corresponding to summer/autumn fluxes. The gradational contact between light and overlying dark laminations is due to slow changes in the biological and sedimentological inputs, while the sharp contact between dark and overlying light laminations is due to the winter hiatus as annual sea ice re-forms. These findings support the interpretation of an annual light–dark couplet.

Sublaminae

Terrigenous laminae may be interrupted by sublaminae that represent events of rapid biogenic export during summer that dilute the terrigenous fraction. The rhizosolenoids sublaminae are encountered at the bottom of the dark laminations, therefore occurring at the beginning of summer season. They demonstrate nutrient limitation above a well-defined pycnocline that enhances their development to the detriment of other species. Nutrient limitation may be linked to a pulsed input of oligotrophic warmer water as evidenced in the Mac Robertson Shelf (Stickley *et al.*, 2005). The abruptness of the Rh events probably records punctual pycnocline breakdown. P sublaminae, present throughout dark laminations, may indicate short bloom events in response to renewal of the nutrient pool via pulsed resurgence of deep waters. Ta sublaminae, generally found at the end of the summer/autumn season, certainly indicate an environmental stress such as decrease in light level and increase in salinity when sea ice returns (Leventer *et al*., 2002; Maddison *et al*., 2005; Stickley *et al*., 2005). Closer to the Adélie Coast, similar sublaminae of nearly monospecific *Porosira glacialis* RS are found to interrupt dark summer laminations (Maddison, 2005). Although both species are thought to have similar growth requirements (Stickley *et al*., 2005) and forecast the autumn/winter transition, we show here that *P. glacialis* may thrive at colder temperatures and higher sea ice cover than *T. antarctica*, in agreement with their occurrence in surface sediments (Armand *et al*., 2005). Diatom census counts evidence anti-correlated occurrences of these two species in core MD03-2601 during the Holocene (data not shown) and ascertain the dominance of *T. antarctica* over *P. glacialis* in the TS.

The three above-described sublaminae types record spring/summer transition (Rh), punctual intense summer blooms (P) and autumn/winter transition (Ta). The distribution of the sublaminae may provide information on atmospheric and oceanic shifts and on sea ice seasonality at the annual scale.

A model of lamina deposition

We developed a schematic model to explain the climatic and oceanic conditions leading to the deposition of the laminations (Figure 6). At the beginning of spring, sea ice starts to melt but a large extent still limits continental input to the water column.

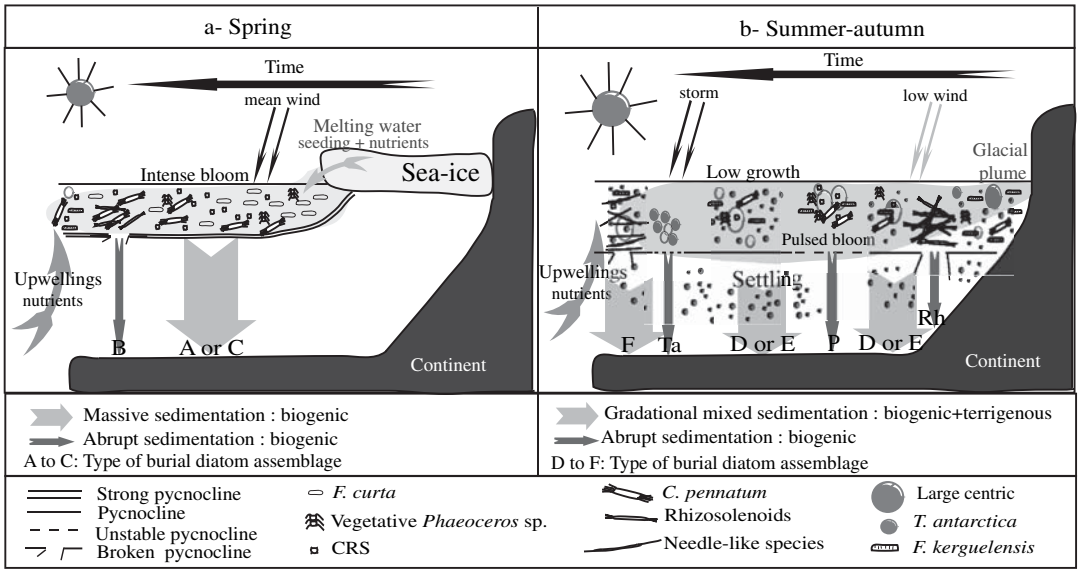

Figure 6 Conceptual model for the deposition of the different laminations and sublaminae recorded in core MD03-2601 for the spring season (a) and the summer–autumn season (b)

Sea ice melting creates strong water column stratification while supplying diatoms and macro- and micronutrients to the surface waters. The beginning of spring is also a time of decrease in the wind regime, of increase in light levels and of high nutrient content in response to the winter overturning. These factors create a favourable environment supporting an intense bloom of cryophilic pennate diatoms and *Chaetoceros* species. As spring advances, the reduction of sea ice influence and the intense nutrient uptake eventually cause CRS formation. Meanwhile, *C. pennatum* and rhizosolenoids slowly build up high biomass at the well-defined pycnocline. They eventually settle after cell senescence or after episodic pycnocline breakdown. In the Antarctic Peninsula, similar laminations have been interpreted to represent autumn mass sedimentation of diatoms that have grown during the period of summer stratification. Summer stratification is promoted by reduced wind activity and the local 'island effect' (Amos, 1987; Huntley *et al.*, 1987). In our study area, more oceanic and more chaotic atmospheric conditions (King and Turner, 1997) conducting to less stable surface water layer, explain episodic export events early in the season. High spring primary production in the form of successive diatom blooms and low detrital supply produces thick biogenic spring laminae.

As summer approaches, light increases and sea ice disappears, driving a transitional diatom assemblage characterized by the appearance of the open water species *F. kerguelensis* and of centric species, mixed with cold water species. At the beginning of summer, punctual pycnocline disruption leads to pulsed exports of rhizosolenoids, imprinted by thin sublaminae. Dilution of sea ice meltwater reduces water column stratification and increases the depth of the pycnocline. The summer light levels are maximum and nutrient content is maintained via MCDW upwelling. These conditions lead to the development of mixed diatom communities primarily dominated by *F. kerguelensis*, while centric species that present a slower growth rate may become co-dominant as the summer develops. A slower but longer diatom growth during summer than during spring is inferred from the higher silicification degree of *C. pennatum*, vegetative *Phaeoceros* sp. and *Fragilariopsis* specimens. The biogenic sedimentation is, however, lower than during spring which, coupled with increased glacial runoff, enables the concomitant settling of terrigenous particles from overflow glacial plumes (Leventer *et al.*, 2002; Finocchiaro *et al.*, 2005). Events of high productivity during summer dilute the terrigenous supply and are recorded as P sublaminae. During autumn, light level decreases, storm activity increases and sea ice returns, thus stimulating the formation of *T. antarctica* that may even lead to Ta sublaminae when the export is rapid.

Interannual variability

While TSs represent snapshots of only a few years that may be lost in the centennial to millennial climate variability, it is attractive to compare the two sequences in term of diatom assemblages. The difference in terrigenous content between the two sections is not conclusive. Section 5 from the Neoglacial period shows expanded spring laminations, dominated by *F. curta*, and reduced summer laminations (Figure 3a). Section 13 from the Hypsithermal period shows reduced spring laminations, dominated by *F. rhombica*, and expanded summer laminations (Figure 3b). These findings demonstrate cooler conditions during the period covered by TS 1–3 than during the period covered by TS 4–6, with late sea ice break up and early sea ice return during the Neoglacial.

Superimposed on the climatic trends, a strong variability in lamination thickness and diatom composition is encountered within each sequence of TS. In section 5, spring laminations of years 1–5 appear much thicker than spring laminations of years 6–11 (Figure 3a) indicating greater diatom productivity in relation to more stable and favourable environmental conditions. This is further confirmed by the reccurence of transitional laminae at the spring/summer transition in years 7–10, which possibly depicts enhanced wind activity during this period. The occurrence of assemblage type B at the beginning of the spring season instead of assemblage type A (Figure 3a) may result from more important injection of oligotrophic warmer water (Stickley *et al.*, 2005) may be resulting in earlier sea ice waning. In section 13, diatom assemblages and succession are more complex during years 1–3 than during years 4–5. Annual sedimentation rate is also reduced, especially because of thinner summer laminations, and many sublaminae are present during years 1–3 (Figure 3b). These findings again argue for less stable conditions during this period that reduced the overall diatom productivity. Lower productivity may also be related to lower nutrient input, as shown by events of greater CRS occurrence and higher silicification degree, may be in relation

to iron limitation (Hutchins and Bruland, 1998), or to earlier return of sea ice in late summer as shown by the Ta sublaminae (Figure 3b).

While TSs represent snapshots of a few years in 'cold' and 'warm' periods, they argue for strong environmental changes in nutrient supply and sea ice cover with a period of 3–5 years. At these latitudes, sea ice seasonal waning and waxing is strongly dependent upon the Antarctic Circumpolar Trough position (Enomoto and Ohmura, 1990). It is therefore attractive to link the observed changes in environmental conditions to the Antarctic Dipole that present a similar 4–5 years cyclicity (Yuan, 2004). Investigation of longer sequences of sediment fabric may help to confirm or refute this hypothesis.

Conclusions

Preliminary investigation of core MD06-2301 from the Adélie Trough illustrates the presence of laminated sedimentary layers that record seasonal and subseasonal diatom productivity and lithic input. Light laminae are mainly biogenic layers with co-dominance of cryophilic *Fragilariopsis* species and CRS. Light laminae correspond to the spring season. Dark laminations show a mixture between terrigenous particles and complex diatom assemblages dominated by *F. kerguelensis* and large centric species. Dark laminae represent the summer/autumn season. Variations in lamination thickness and in diatom assemblage types reveal a strong interannual variability that results from the interplay of sea ice, glacial runoff and oceanic currents in response to interactions between the atmosphere, ocean and cryosphere. These local to regional changes are possibly connected to the global sea ice cycle around Antarctica via the Antarctic Dipole. Further investigations of longer sections will provide a unique tool to document local to global Antarctic climate variability and cyclicity during the Holocene period at the seasonal resolution.

Acknowledgements

We thank Eleanor Maddison, Jacques Giraudeau and William Fletcher for constructive discussions. We also thank Jenny Pike, Amy Leventer and Lloyd Burckle whose helpful reviews greatly improved the manuscript. We personally thank people from *Images* X (CADO) cruise and from NSF-funded NBP0101 cruise for data and suggestions concerning the D'Urville Trough. Financial support for this study was provided by TARDHOL project through the national PNEDC Program (INSU-CNRS), and the Institut Paul Emile Victor (IPEV). This is an EPOC contribution No. 1597.

References

Amos, A.F. 1987: RACER: physical oceanography of the western Bransfield Strait. *Antarctic Journal of the United States* 22, 137–40.

Armand, L.K., Crosta, X., Romera, O. and **Pichon, J.J.** 2005: The biogeography of major diatom taxa in Southern Ocean sediments: 1. Sea ice related species. *Palaeogeography, Palaeoclimatology, Palaeoecology* 223, 93–126.

Bahk, J.J., Yoon, H.I., Kim, Y., Kang, C.Y. and **Bae, S.H.** 2003: Microfabric analysis of laminated diatom ooze (Holocene) from the eastern Bransfield Strait, Antarctica Peninsula. *Geosciences Journal* 7, 135–42.

Beucher, C., Tréguer, P., Corvaisier, R., Hapette, A.M. and **Elskens, M.** 2004: Production and dissolution of biosilica, and changing microphytoplankton dominance in the Bay of Brest (France). *Marine Ecology Progress Series* 267, 57–69.

Bindoff, N.L., Williams, G.D. and **Allison, I.** 2001: Sea ice growth and water mass modification in the Mertz Glacier Polynya during winter. *Annals of Glaciology* 33, 399–406.

Bond, G., Cromer, B., Beer, J., Muscheler, R., Evans, M.N., Showers, W., Hoffman, S., Lotti-Bond, R., Hajdas, I. and **Bonani G.** 2001: Persistent solar influence on North Atlantic climate during the Holocene. *Science* 294, 2130–36.

Crawford, R.M. 1995: The role of sex in the sedimentation of a marine diatom bloom. *Limnology and Oceanography* 40, 200–204.

Crosta, X., Pichon, J.J. and **Labracherie, M.** 1997: Distribution of *Chaetoceros* resting spores in modern peri-Antarctic sediments. *Marine Micropaleontology* 29, 238–99.

Crosta, X., Crespin, J., Billy, I. and **Ther, O.** 2005: Major factors controlling Holocene $\delta^{13}C_{org}$ changes in a seasonal sea ice environment, Adélie Land, East Antarctica. *Global Biogeochemical Cycles* 19, GB4029, DOI: 10.1029/2004GB002426.

de Menocal, P., Ortiz, J., Guilderson, T. and **Sarnthein, M.** 2000: Coherent high- and low-latitude climate variability during the Holocene warm period. *Science* 288, 2198–202.

Enomoto, H. and **Ohmura, A.** 1990: The influences of atmospheric half-yearly cycle on the sea ice extent in the antarctic. *Journal of Geophysical Research* 95, 9497–511.

Escutia, C., Warnke, D., Acton, G.D., Barcena, A., Burckle, L., Canals, M. and **Frazee, C.S.** 2003: Sediment distribution and sedimentary processes across the Antarctic Wilkes Land margin during the Quaternary. *Deep-Sea Research II* 50, 1481–508.

Finocchiaro, F., Langone, L., Colizza, E., Fontolan, G., Giglio, F. and **Tuzzi, E.** 2005: Record of the early Holocene warming in a laminated sediment core from Hallett Bay (Northern Victoria Land, Antarctica). *Global and Planetary Change* 45, 193–206.

Francus, P. 1998: An image-analysis technique to measure grain-size variation in thin sections of soft clastic sediments. *Sedimentary Geology* 121, 289–98.

Francus, P., Keimig, F. and **Besonen, M.** 2002: An algorithm to aid varve counting and measurement from thin-sections. *Journal of Paleolimnology* 28, 283–86.

Fryxell, G.A. and **Hasle, G.R.** 1971: *Corethron criophilum* castracane: its distribution and structure. *Antarctic Research Series* 17, 335–46.

Garrison, D.L., Buck, K.R. and **Fryxell, G.A.** 1987: Algal assemblages in Antarctic pack ice and in ice-edge plankton. *Journal of Phycology* 23, 564–72.

Harris, P.T. 2000: Ripple cross-laminated sediments on the East Antarctic Shelf: evidence for episodic bottom water production during the Holocene? *Marine Geology* 170, 317–30.

Harris, P.T. and **Beaman, R.J.** 2003: Processes controlling the formation of the Mertz Drift, George Vth continental shelf, East Antarctica: evidence from 3.5kHz sub-bottom profiling and sediment cores. *Deep-Sea Research II* 50, 1463–80.

Hodell, D.A., Shemesh, A., Crosta, X., Kanfoush, S., Charles, C. and **Guilderson, T.** 2001: Abrupt cooling of Antarctic surface waters and sea ice expansion in the South Atlantic sector of the Southern Ocean at 5000 cal yr BP. *Quaternary Research* 56, 191–98.

Huntley, M.E., Niiler, P., Holm-Hansen, O. and **Karl, D.M.** 1987. RACER: an inter-disciplinary field study. *Antarctic Journal of the United States* 22, 135–37.

Hutchins, D.A. and **Bruland, K.W.** 1998: Iron-limited diatom growth and Si:N uptake ratios in a coastal upwelling regime. *Nature* 393, 561–64.

Ingólfsson, O., Hjort, C., Berkman, P.A., Björck, S., Colhoun, E., Goodwin, I.D., Hall, B., Hirakawa, K., Melles, M., Möller, P. and **Prentice, M.L.** 1998: Antarctic glacial history since the last glacial maximum: an overview of the record on land. *Antarctic Science* 10, 326–44.

Jansen, J.H.F., Van der Gaast, S.J., Koster, B. and **Vaars, A.J.** 1998: CORTEX, a shipboard XRF-scanner for element analyses in split sediment cores. *Marine Geology* 151, 143–53.

Jones, P.D., Marsh, R., Wigley, T.M.L. and **Peel, D.A.** 1993: Decadal timescale links between Antarctic Peninsula ice core oxygen-18 and temperature. *The Holocene* 3, 14–26.

Kemp, A.E.S., Pearce, R.B., Koizumi, I., Pike, J. and **Rance, S.J.** 1999: The role of mat forming diatoms in formation of the Mediterranean Sapropels. *Nature* 398, 57–61.

Kemp, A.E.S., Pike, J., Pearce, R.B. and **Lange, C.B.** 2000: The 'fall dump': a new perspective on the role of a shade flora in the annual cycle of diatom production and export flux. *Deep-Sea Research II* 47, 2129–54.

King, J.C. and **Turner, J.** 1997**:** *Antarctic meteorology and climatology*. Cambridge Atmospheric and Space Science Series. Cambridge University Press, 409 pp.

King, J.C., Turner, J., Marshall, G.L., Connolley, W.M. and **Lachlan-Cope, T.A.** 2003: Antarctic Peninsula climate variability and its causes as revealed by analysis of instrumental records. *Antarctic Peninsula Climate Variability* 79, 12-1–12-4.

Leventer, A. 1991: Sediment trap diatom assemblages from the northern Antarctic Peninsula region. *Deep-Sea Research* 38, 1127–43.

—— 1992: Modern distribution of diatoms in sediments from the George V coast, Antarctica. *Marine Micropaleontology* 19, 315–32.

Leventer, A. and **Dunbar, R.B.** 1987: Diatom flux in McMurdo Sound, Antarctica. *Marine Micropaleontology* 12, 49–64.

Leventer, A., Domack, E., Barkoukis, A., McAndrews, B. and **Murray, J.** 2002: Laminations from the Palmer Deep: a diatom-based interpretation. *Paleoceanography* 17, 1–15.

Leventer, A., Domack, E., Dunbar, R., Pike, J., Stickley, C., Maddison, E., Brachfeld, S., Manley, P. and **McClennen, C.** 2006: East Antarctic margin marine sediment record of deglaciation. *GSA Today* in press.

Maddison, E.J. 2005: Seasonally laminated Late Quaternary Antarctic sediments. Ph.D. thesis, Cardiff University, 218 pp.

Maddison, E.J., Pike, J., Leventer, A. and **Domack, E.W.** 2005: Deglacial seasonal and sub-seasonal diatom record from Palmer Deep, Antarctica. *Journal of Quaternary Science* 20, 435–46.

Massom, R.A., Harris, P.T., Michael, K.J. and **Potter, M.J.** 1998: The distribution and formative processes of latent-heat polynyas in East Antarctica. *Annals of Glaciology* 27, 420–26.

Masson, V., Vimeux, F., Jouzel, J., Morgan, V., Delmotte, M., Ciais, P., Hammer, C., Johnsen, S., Lipenkov, Y., Mosley-Thompson, V.E., Petit, J.-R., Steig, E.J., Stievenard, M. and **Vaikmae, R.** 2000: Holocene climatic variability in Antarctica: what can be inferred from 11 ice core isotopic records? *Quaternary Research* 54, 348–58.

McMinn, A. and **Hodgson, D.** 1993: Seasonal phytoplankton succession in Ellis Fjord, eastern Antarctica. *Journal of Planktonic Research* 15, 925–38.

Migeon, S., Weber, O., Faugeres, J.-C. and **Saint-Paul, J.** 1999: SCOPIX: A new X-ray imaging system for core analysis. *Geo-Marine Letters* 18, 251–55.

Moran, S.B. and **Moore, R.M.** 1992: Kinetics of the removal of dissolved aluminium by diatoms in seawater: a comparison with thorium. *Geochimica et Cosmochimica Acta* 56, 3365–74.

NGICP members 2004: High-resolution record of Northern Hemisphere climate extending into the last interglacial period. *Nature* 431, 147–51.

Nielsen, S.H.H., Koç, N. and **Crosta, X.** 2004: Holocene climate in the Atlantic sector of the Southern Ocean: controlled by insolation or oceanic circulation? *Geology* 32, 317–20.

Pike, J., Moreton, S.G. and **Allen, C.A.** 2001: Data report: microfabric analysis of postglacial sediments from Palmer Deep, Western Antarctic Peninsula. In Barker, P.F., Camerlenghi, A., Acton, G.D. and Ramsay, A.T.S., editors, Proceedings of the ODP. *Science Research* 178, 1–17. Retreived 9 April 2005 from http://www.odp.tamu.edu/publications/178_SR/VOLUME/CHAPTERS/SR178_18.PDF

Presti, M., De Santis, L., Busetti, M. and **Harris, P.T.** 2003: Late Peistocene and Holocene sedimentation on the George V Continental Shelf, East Antarctica. *Deep-Sea Research* II 50, 1441–61.

Rathburn, A.E., Pichon, J.-J., Ayress, M.A. and **De Deckker, P.** 1997. Microfossil and stable-isotope evidence for changes in the late Holocene paleoproductivity and paleoceanographic conditions in the Prydz Bay region of Antarctica. *Palaeogeography, Palaeoclimatology, Palaeoecology* 131, 485–510.

Riaux-Gobin, C., Poulin, M., Prodon, R. and **Treguer, P.** 2003: Land-fast ice microalgal and phytoplanktonic communities (Adélie land, Antarctica) in relation to environmental factors during ice break-up. *Antarctic Science* 15, 353–64.

Rignot, E. and **Jacobs, S.S.** 2002: Rapid bottom melting widespread near Antarctic ice sheet grounding lines. *Science* 296, 2020–23.

Saporta, G. 1990: *Probabilités analyse des données et statistique*. Editions technip.

Schweitzer, P.N. 1995: *Monthly averaged polar sea ice concentration*. U.S. Geological Survey Digital Data Series.

Stickley, C.E., Pike, J., Leventer, A., Dunbar, R.B., Domack, E.W., Brachfeld S.A., Manley, P. and **McClennan, C.** 2005: Deglacial ocean and climate seasonality in laminated diatom sediments, Mac Robertson Shelf, East Antarctica Margin. *Palaeogeography, Palaeoclimatology, Palaeoecology* 227, 290–310.

Taylor, S.R. and **Mclennan, S.M.** 1985: *The continental crust: its composition and evolution*. Blackwell Science, 312 pp.

Van Bennekom, A.J., Jansen, J.H.F., Van der Gaast, S.J., Van Iperen, J.M. and **Pieters, J.** 1989: Aluminium-rich opal: an intermediate in the preservation of biogenic silica in the Zaire (Congo) deep-sea fan. *Deep-Sea Research* 36, 173–90.

Yarincik, K.M. and **Murray, R.W.** 2000: Climatically sensitive eolian and hemipelagic deposition in the Cariaco Basin, Venezuela, over the past 578,000 years: results from Al/Ti and K/Al. *Paleoceanography* 15, 210–28.

Yuan, X. 2004: ENSO-related impacts on Antarctic sea ice: a synthesis of phenomenon and mechanisms. *Antarctic Science* 16, 415–25.

Zaragosi, S., Bourillet, J-F., Eynaud, F., Toucanne, S., Denhard, B., Van Toer, A. and **Lanfumey, V.** 2006: The impact of the last European deglaciation on the deep-sea turbidite systems of the Celtic-Armorican margin (Bay of Biscay). *Geomarine Letters* in press.

Zielinski, U. and **Gersonde, R.** 1997: Diatom distribution in Southern Ocean surface sediments (Atlantic sector): implications for paleoenvironmental reconstructions. *Palaeoceanography, Palaeoclimatology, Palaeoecology* 129, 213–50.